# A Comparative Study on Assessment of Carotid Artery Using Various Techniques


**S. Mounica, B. Thamotharan, and S. Ramakrishnan**

## 1 Introduction

Ultrasound imaging performs the estimation of the atherosclerotic concern in the carotid artery. For disclosure at recent point of atherosclerosis, IMT is the most widely used parameter. It is described by the gap among the lumen-intima interface (LII) to the media-adventitia interface (MAI). The major role that plays an initiation and progression of atherosclerosis is the increased levels of cholesterol for specific low-frequency lipoproteins. In prevention of atherosclerosis, high-frequency lipoproteins are treated to be favorable. A quick and easy method for anazlysing inflammatory status is the Neutrophil-to-Lymphocyte Ratio (NLR), evaluated as the ratio of exact neutrophil count to exact lymphocyte count [6]. Carotid artery occlusion was resolved if embolic material was identified in the artery wall by lengthwise and declination ultrasound without color flow signal and the Doppler spectrum. Using magnetic resonance imaging, the associations between atherosclerotic plaque features and the deviations in symptomatic and asymptomatic carotid atherosclerotic plaques (Fig. 1).

S. Mounica · B. Thamotharan (✉) · S. Ramakrishnan
School of Computing, SASTRA Deemed-to-Be-University, Thanjavur, India
e-mail: srk@ict.sastra.edu



S. Smys et al. (eds.), *New Trends in Computational Vision and Bio-inspired Computing*, https://doi.org/10.1007/978-3-030-41862-5_64

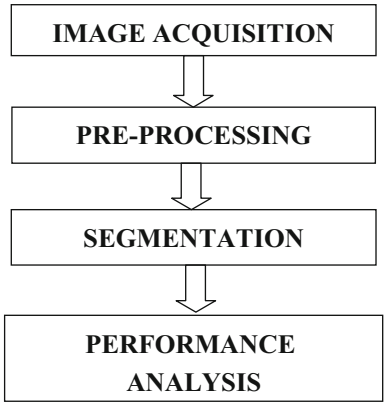


**Fig. 1** Overall workflow of a system

## 2 Image Acquisition

### *2.1 Carotid Endarterectomy*

From asymptomatic and symptomatic patients, plaques were detached by endarterectomy and to show different histological vulnerability it is divided into three different regions: A, upstream of the maximal stenosis; B, a station for maximal narrowing; C, ensuing of the maximal narrowing [1]. When the fundamental narrowing was detached in an uninterrupted manner, endarterectomy was performed. Immunohistochemistry analyzes plaque content and multiplex technology content by plaque cytokine. It was efficiently greater in plaques resulted from the patients with diabetes and a high fibromodulin solution was grouped with a greater extent of checkup cerebrovascular functions [11], although no alike grouped were examine for lumican. Fibromodulin solution also combination with plaque lipids and many proinflammatory cytokines (Fig. 2).

### *2.2 Doppler Ultrasound*

The development of micro embolic signals (MES) on transcranial Doppler is the reparative comparison ultrasound discovery of the cervical carotid arteries that were grouped during the disclosed of the arteries in CEA, the assumption efficiency is compared to contrast-enhanced ultrasound solution of a certain of the gray-scale median (GSM) [2]. The extent of establishment of carotid atherosclerotic plaque were associated on carotid intima-media thickness (IMT). The visualization of blood flow velocities and the proximal wall of ICA allows imaging of color duplex ultrasound. This quick noninvasive method which does not require contrast administration offers a dynamic view of vessels [17]. The best Doppler parameter is the Peak systolic velocity (PSV) used for computing carotid artery extent of stenosis.

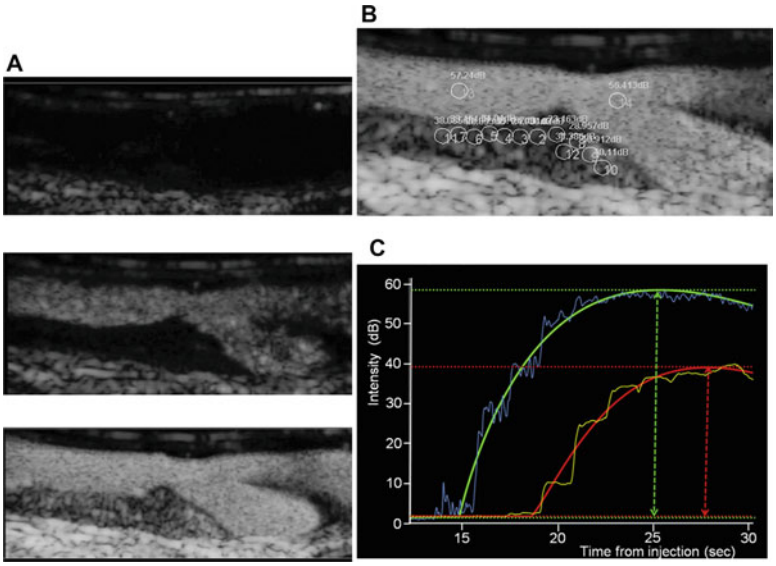


**Fig. 2** Carotid enterectometry [14]

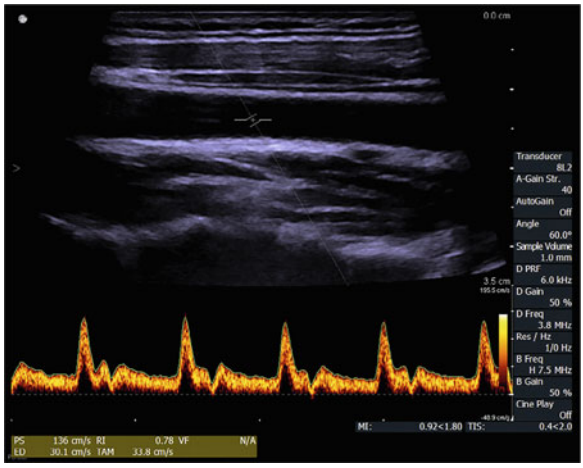


**Fig. 3** Standard scanner using spectral Doppler ultrasound

The Doppler calculation of the middle third of common carotid artery was fixed with a longitudinal view, with specimen quantity in the center of the vessel (Fig. 3).

## 2.3 B Mode Ultrasound

Coupled plasma mass spectrometry analyses the Cadmium level in blood by inductive method. For the occurrences of plaque, the "window" compressing 3 cm of the distal common carotid artery, the bifurcation, and 1 cm of the internal and external carotid artery was scanned with consequence field in right common carotid artery [20]. The structures for their identification and picture contradiction function of lumen and the consequences in carotid artery are correlated to other tissues. For speckle noise removal, the intake picture is detected using morphologic operative and sequenced by an anisotropic dispersal drain that presents the appropriate ultrasound values corresponds to the artery. To describe two initial curves, the information obtained is used, i.e. one corresponds to the lumen and the alternative one corresponds to consequence ends. This method is done in the Chan-Vese level set model.

## 2.4 Computed Tomography

The information of the vascular tree, the extent of stenosis, and the occurrence of calcified plaque are provided by CT. The limitation in CT involves soft plaque characterization. The histology is available only if the tissue is excised but still, it is the gold standard. The potential for the US is validated with diagnosis and X-ray calculated tomography (CT) as a technique for non-invasive pictures in the carotid artery [4]. For the assessment of WMC (white matter changes), pre-interventional cerebral CT/MRI is used. A actual particular sensitive sign of arterial examination on CT Angiography is the broad eccentric lumen occupied by crescent-shaped mural narrowing and thin annular establishment (Fig. 4).

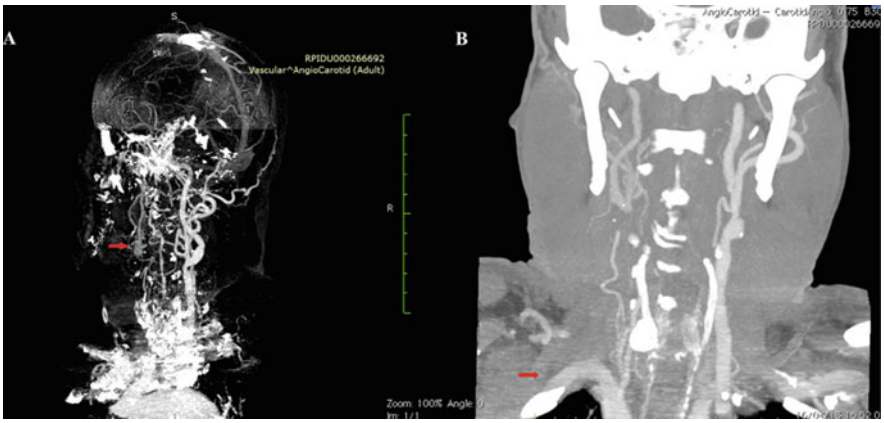


**Fig. 4** Computed tomography

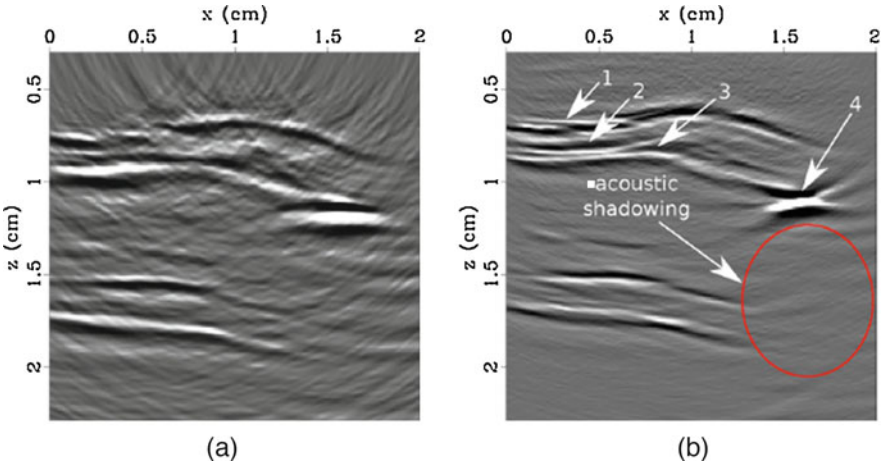


**Fig. 5** Standard scanner using spectral Doppler ultrasound

## *2.5 Reflection-Mode all-Optical Laser-Ultrasound (LUS)*

This imaging method is to evaluate high-decision, non-relationship, non-ionizing pictures of the carotid artery block and concretion as shown in Fig. 5. For soft recovery, calculation and user-vulnerable data recovery for high occurrence, all-optical LUS is used. When compared with confocal LUS to confocal LUS, the inner row of the artery wall, growth of the vessel, and concretion are analysed with greater decision and decreased artifacts [5].

## *2.6 3D Ultrasound Imaging*

The optical motion tracking technology is a freehand 3D ultrasound imaging technique. L-frame calibration determines 3D space coordinates. The eight digital cameras detect using the positions of an L-frame, which could provide a volume of 3D view when it captures simultaneously. The exhaustive stenosis function lacks the determination of the plaque characteristics and the vessel boundary and the imaging of stenosis move towards the inbound flow can be given. The different techniques that performs 3D imaging of carotid stenosis involves as shown in Fig. 6: (1) The US B-Mode towards the vessel wall parenchymal (CT/MRI) imaging the 3D restructure of internal carotid artery plaque structure and (2) 3D restructure in internal residual lumen, visioned by Power Doppler or with any imaging methods [16].

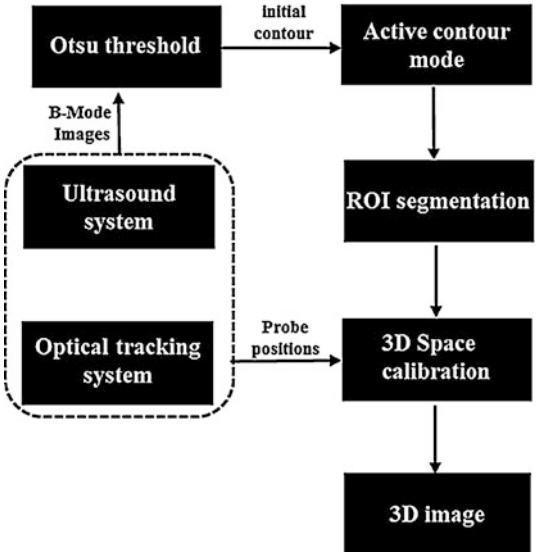


**Fig. 6** 3D ultrasound imaging

## *2.7 MRI*

A state-of-the-art Diffusion Tensor Imaging (DTI) carotid plaques were visualised with ex-vivo using high magnetic field MRI scanner. The 3-D data sets is provided by MRI with isotropic or nearly isotropic voxels that are highly reproducible, self-reliant with size angle and less vulnerable on the experience of the operative. Using multiple parameter MRI consisting of the time of flight (TOF), T1-weighted, and T2-weighted sequences, plaque appearance like new hemorrhage, lipid-rich necrotic core, intimal calcification, and fibrous tissue can be determined. The accurate relationship among thick and a thin (<150 $\mu$m) coarse cover is insufficient in the resolution of MRI. The MRI fat/water separation method is quantitatively to evaluate the potential, calles as repeated disintegration of water and fat with parallel similarity and least squares estimation (IDEAL) to combine and increase the disadvantages of previous methods for the assessment of hemorrhage and lipids in carotid artery plaques. For the MCW assessment the MRI protocol has 3 scans: 3D Time-of-Flight (3D-TOF); 2D T1-weighted black blood fast spin echo (T1W-BB-FSE); and 2D T2-weighted black blood fast spin echo (T2WBB- FSE) imaging. Fat/water IDEAL imaging was done by a 2D T1W-BB-FSE pulse arrangement [7].

# 3 Pre-Processing

## *3.1 Pre-Processing Techniques*

Pre-processing removes noise and improves the image contrast, its accuracy mainly impacts the results of segmentation. Weak boundaries and unrelated parts can be removed using pre-processing. Noise can get introduced into an image during storage, transmission, processing or it might be present when the image was created. It can be removed through various pre-processing techniques. Different pre-processing techniques discussed in this paper include:

- Mean filter
- Median filter
- Adaptive median filter
- Gaussian filter
- Salt and pepper noise
- Speckle noise

### 3.1.1 Mean Filter

Mean filter or Average filter is a low pass filter where the average value is placed as the centre value for every position. The aim of using a mean filter is to improve the appearance of an image for interpretation. Mean filter is a linear filter or a convolution filter which can be represented as a matrix. It moves through the image, pixel by pixel by replacing the centre value by the mean value of the neighbouring pixels.

### 3.1.2 Median Filter

Median filtering is a non-linear filtering technique that decreases *salt and pepper noise* while preserving the sharpness of the edges in an image. This works better than the mean filter as it removes noise, while mean filter spreads the noise evenly. Median is the middle value of its neighbouring pixels where half of the neighbour pixels are smaller and half are larger. The disadvantage of median filter is that it treats noise and fine detail in a similar manner and hence it removes fine details also.

### 3.1.3 Adaptive Median Filter

This filter preserves the edges by lessening the bends and it traces out which pixel is influenced by impulse noise by performing spatial handling [9]. Adaptive median filtering is an advanced technique when compared to median filtering. The pixels

affected by impulse noise can be determined by performing spatial processing. In an Adaptive Median Filter, each pixel in the image is compared to its surrounding neighbour pixels and based on that the pixels are classified as noise. Median filter can perform well only until the spatial density of the impulse noise is not large but adaptive median filter can work even if it is large.

### 3.1.4 Wiener Filter

Image with lower MSE value has better visual quality and wiener filter lowers this MSE value during noise smoothing and inverse filtering. It does not alter the mammogram image but improves its quality. It can simultaneously remove noise and invert blurring. It depends on the *Fourier cycle* and requires only a short computational time to identify a solution to a problem [8].

### 3.1.5 Gaussian Filter

A Gaussian filter is a non-uniform low pass filter with Gaussian function using which the low and high signal distortion can be controlled. An image can be smoothened and interpolated simultaneously using Gaussian filter and the variance, $\sigma^2$, should be $\geq 1$. At location (y, x), for non-integer row index y and column index x, the estimated intensity is an average of local pixel values, weighted by the Gaussian density function in Eq. (1):

$$g(y,x) = \sum_{i=[y-3\sigma]}^{i=[y+3\sigma]} \sum_{j=[x-3\sigma]}^{j=[x+3\sigma]} \left( \frac{f_{ij}}{2\psi^2} \right) \exp \left( \frac{\left\{ -\left\{ (i-y)^2 + (j-x)^2 \right\} \right\}}{2\sigma^2} \right) \tag{1}$$

### 3.1.6 Salt and Pepper Noise

It is also called as impulse noise and that is seen on images as a form of noise. The image signal caused by noise is usually a pointed and abrupt disruption. The white and black pixels is presented by its own scant occurring. Nikolova et al. show a median filter or a morphological filter as an active blast removal method for this type of noise

### 3.1.7 Speckle Noise

The incidental values can be modeled by multiplying pixel values of an image. Rajabi et al. show that incidental fluctuation is a result that returns signal from an object. A single image processing element is no bigger than this. It increases the local area level of a mean grey. The filtering techniques that are used is mean and median filtering [9].

## 4 Segmentation

Active contour is an important method in image segmentation. *Edge based* and *region-based* methods are active contour methods. Chan-Vese models can be used for segmenting noisy images. Though Chan-Vese level set segmentation provides best recall, regions of interest cannot be segmented accurately in all cases. Identification process for lesions should be done only in the relevant areas of the image. The efficiency of this system strongly depends on the accuracy of result segmentation. Segmentation can be done in many ways few of the method are compared with their efficiency.

### *4.1 Active Contour*

The Otsu's method segments the picture of the basic contour exposed and it is generated semi-automatically. The ACM algorithm provides the initial contours. This design encounters the curve of the carotid artery and sectors the artery border. The picture can be coordinated on the basis of probe position at the end in 3D overall correspondent area. To find the threshold value of the picture for visualizing the initial contour function is first used by Otsu's algorithm [10].

### *4.2 Deep Learning*

The broad linear composed of numerous transforming thickness is the extraction of high-level representations of the input that are attempted to the larges appropriate particular information work. A attribute of grouping nonlinear transforming group that transforms an image into statistical information. To restore common imaging appearance (e.g., wavelets, spatial textures, statistical moments) with transforming row, deep learning denotes which are added complicated along with extra particular statistics and work. It also leads to an excellent handling of data and enhanced prognosis influence function. CNN's are categories of deep learning construction values of convolutional filters (i.e., kernels of differing content) at any row to

**Table 1** Deep learning approach validation for metadata of the plaques

| Difference | Start | End |
|---|---|---|
| Size of plaque ($mm^2$) | 5.8 | 176.9 |
| Percentage of lipid core (%) | 1.8 | 83.1 |
| Percentage of fibrous tissue (%) | 14.6 | 68.9 |
| Percentage of calcified tissue (%) | 2.7 | 85.2 |
| Maximal intensity | 170 | 275 |

abstract current appearance from exercise pictures that are appropriate for the picture perception work. A Sequence of a particular auto-encoder set of designs that experiments the classic extra unreal and appropriate portrayal of data with many non-linear revolution, by a process of its construction is emerged from Deep learning (Table 1) [12].

### *4.3 Snake Algorithm*

The finest resemblance in snake at the curve of plaques, this design is occupying the operation of cubic spline responsibility that allows. To assess the automatic recovery of snake points, the mathematical framework of the spline is used in contrast with those achieved by standard bisection. The design integrated is normalization, speckle reduction filtering, bisection approach, with initialization positioned on the blood movement picture, were proved in the background of bispatial (2-D) lengthwise pictures of carotid plaques [13].

### *4.4 Level Set Segmentation Algorithm*

The horizontal-arranged delineation design performs an flexible, robust, active, suitable skilled and actual algorithm can be worned in much scientific imaging and disorder function through the detached bisection of ROIs defined by nonlinear line curves. The commonly-arranged design is defined by a folded loop or curve described by,

$$\Gamma = \left\{ (x, y :) \ \varphi (x, y) = \right\} 0 \tag{2}$$

where (x, y) is the growth origin mark of the curve and φ(x, y) is the aligned fixed, of all marks be of the fastened curve. The fastened curving Γ also was known as the loop multiplication is contained by the definite objective φ which is determined by the confident intervals of the independent locality of the curve (Table 2).

**Table 2** summary of the pixel-based accuracy by SVM techniques

| | Median | Mean | Std | Min | Max | %best result |
|---|---|---|---|---|---|---|
| Single-scale SVM | 1.76 | 1.81 | 1.14 | 1.31 | 1.47 | 9.7 |
| Multiscale SVM | 1.80 | 1.09 | 1.17 | 1.50 | 1.04 | 13.9 |
| Proposed CNN | 1.90 | 1.85 | 1.19 | 1.76 | 1.67 | 79.8 |

## 5 Performance Analysis

### *5.1 Pulse Wave Velocity Assessment (PWV)*

The momentum by which the vibration movement proliferates over the arterial tree is given by the arterial stiffness parameter. The rate at which the width of two position and the change in appearance of the vibration movement at these two positions. The assessment locations in PWV denotes the rigidity of the aorta is the most common femoral arteries used [14]. The Moens-Korteweg equation shows the thin-walled arteries that is associated to its flexible properties.

$$PWV = \sqrt{\frac{E_{inc} \cdot h}{2r\rho}} \tag{3}$$

where $E_{inc}$ = incremental elastic modulus of the vessel wall, $h$ = wall thickness, $r$ = vessel radius, and un$\rho$ = blood density.

### *5.2 Subject-Specific Mathematical Modeling*

To evaluate the assessment in reproviding the relation among carotid tonometry waveform and distal PVR, three physical models are defined. The relation: a tube-load model augmented with again (TLG), Voigt (TLV), and standard linear solid (TLS) model which is the conducting system identification by locating them to the carotid artery tonometry waveform and distal PVR data collected from many sources.

### *5.3 Nonlinear State-Space Approach: (State of the Art Approach)*

The passage of the CCA wall is a experiment done using the nonlinear state-space equation with a time-variant control signal was build. To resolve the nonlinear state transfer function, the unscented Kalman filter (UKF) was adopted. So, to evaluate the state of the target tissue, which includes the establishment of the motion trajectory of the CCA wall from noisy ultrasound pictures**.** The state transfer function in the state-space equation is evaluated by a nonlinear quasi-periodic function, that is approximated by setting the nonlinear component of carotid dynamics [15].

### *5.4 Intima-Media Thickness*

The echo function and construction of the plaque of the bilateral common carotid arteries, internal carotid arteries, and carotid bulbs were analyzed and used by the Intima-Media Thickness (IMT). From the output of the carotid artery, color Doppler ultrasound, AaCI patients were grouped into IMT normal group (IMT < 1.0 mm), IMT thickening group (1.0 mm $\leq$ local IMT < 1.5 mm), plaque formation group (local IMT $\geq$ 1.5 mm. A fast edge- detection technique is proposed for efficient measurement of the IMT, based on a structured random forest classifier. IMT is calculated by the way of ultrasound scans. To estimate the thickness of artery, the optimal calculated area which finds the set of arterial wall and that make couple of marks on the picture is done during the radiological examination. The distance among the intimal–luminal interface and the medial– adventitial interface, was evaluated in all patients is defined as C-IMT.

### *5.5 Logistic and Linear Regression Models*

Due to its skewed distribution, TPA was log transformed. To analyse the group of its adiposity quantity with the findings of plaque and with measurement scale TPA, logistic and linear regression were used for the plaque performance. With the detection of plaque as an conclusion to examine the group of adiposity with having at least one plaque, a logistic regression method was used. To produce the group between adiposity and plaque burden with no recorded plaque, a log-transformed TPA was used as the conclusion in a linear regression method. To improve the approximation to the normal distribution, TPA was log-transformed. Using a hurdle model, these two are in combination that is equal to with that of logistic regression modeling of the circulation of zero plaque compared with at least one plaque, and the linear regression modeling of the circulation of the non-zero assessment. Regression analysis is used in the group of cardiovascular source and carotid plaque group with plaque burden and lumen volumes.

## 6 Results

To evaluate a proposed method called 3-D US vector flow imaging US observation of the CCA was related with a over-flat MRI arrangement. For normal functions of plaque configuration in carotid ultrasound images, Deep learning approach is used. The results improved when the acceptance of a hugely fluctuating case shows that, the obtained results with the most progressive new method. In most of the cases, it is used in SVM and predefined imaging appearance, with an improvement of 79.5%. The IMT can be calculated as a fully user-independent and reusable way. The main

input and efficiency of the enhanced procedure as follows: a higher intellect and autonomy of the work; the intensity of toughness in the anatomical and involved fluctuation of the ultrasound images; and the unique accuracy and attention for calculation of the IMT.

**Acknowledgement** No patients are involved in this work. We used our own data.

## References

1. Menchón-Lara RM, Sancho-Gómez JL, Bueno-Crespo A. Early-stage atherosclerosis detection using deep learning over carotid ultrasound images. Applied Soft Computing. 2016 Dec 1;49:616–28.
2. Selwaness M, Hameeteman R, Van'tKlooster R, Van den Bouwhuijsen Q, Hofman A, Franco OH, Niessen WJ, Klein S, Vernooij MW, Van der Lugt A, Wentzel JJ. Determinants of carotid atherosclerotic plaque burden in a stroke-free population. Atherosclerosis. 2016 Dec 1;255:186–92.
3. Sulženko J, Pieniazek P. The cardiovascular risk of patients with carotid artery stenosis. Coret Vasa. 2017 Oct 31.
4. Yeom E, Nam KH, Jin C, Paeng DG, Lee SJ. 3D reconstruction of a carotid bifurcation from 2D transversal ultrasound images. Ultrasonics. 2014 Dec 1;54(8):2184–92.
5. Corriere T, Di Marca S, Cataudella E, Pulvirenti A, Alaimo S, Stancanelli B, Malatino L. Neutrophil-to-Lymphocyte Ratio is a strong predictor of atherosclerotic carotid plaques in older adults. Nutrition, Metabolism and Cardiovascular Diseases. 2018 Jan 1;28(1):23–7.
6. Johnson JL, Merrilees M, Shragge J, van Wijk K. All-optical extravascular laser-ultrasound and photoacoustic imaging of calcified atherosclerotic plaque in excised carotid artery. Photoacoustics. 2018 Mar 1;9:62–72.
7. Tat J, Psaromiligkos IN, Daskalopoulou SS. Carotid atherosclerotic plaque alters the direction of longitudinal motion in the artery wall. Ultrasound in Medicine and Biology. 2016 Sep 1;42(9):2114–22.
8. Guo L, Cheng L, He W, Ju Y, Zhao X. Ideal Cardiovascular Health and Incidence of Carotid Plaque among Middle-Aged and Elderly Adults. Journal of Stroke and Cerebrovascular Diseases. 2018 Feb 1;27(2):391–6.
9. Alam J, Hassan M, Khan A, Chaudhry A. Robust fuzzy RBF network based image segmentation and intelligent decision making system for carotid artery ultrasound images. Neurocomputing. 2015 Mar 5;151:745–55.
10. Giannoni MF, Vicenzini E, Sbarigia E, Di Piero V, Lenzi GL, Speziale F. Early ultrasound imaging of carotid arteries in the acute ischemic cerebrovascular patients. Perspectives in Medicine. 2012 Sep 1;1(1–12):108–11.
11. Salem MK, Butt HZ, Choke E, Moore D, West K, Robinson TG, Sayers RD, Naylor AR, Bown MJ. Gene and protein expression of chemokine (cc-motif) ligand 19 is upregulated in unstable carotid atherosclerotic plaques. European Journal of Vascular and Endovascular Surgery. 2016 Oct 1;52(4):427–36.
12. Khosa F, Clough RE, Wang X, Madhuranthakam AJ, Greenman RL. The potential role of IDEAL MRI for identification of lipids and hemorrhage in carotid artery plaques. Magnetic resonance imaging.2017 Dec 5.
13. Oikawa K, Kato T, Oura K, Narumi S, Sasaki M, Fujiwara S, Kobayashi M, Matsumoto Y, Nomura JI, Yoshida K, Terayama Y. Preoperative cervical carotid artery contrast-enhanced ultrasound findings are associated with development of microembolic signals on transcranial Doppler during carotid exposure in endarterectomy. Atherosclerosis. 2017 May 1;260:87–93.

14. Lynser D, Daniala C, Khan AY, Marbaniang E, Thangkhiew I. Effects of dynamic range variations on the Doppler flow velocities of common carotid arteries. Artery Research. 2018 Jun 30;22:18–23.
15. Shimada Y, Oikawa K, Fujiwara S, Ogasawara Y, Sato Y, Narumi S, Kato T, Oura K, Terayama Y, Sasaki M, Fujimoto K. Comparison of Three-Dimensional T1-Weighted Magnetic Resonance and Contrast-Enhanced Ultrasound Plaque Images for Severe Stenosis of the Cervical Carotid Artery. Journal of Stroke and Cerebrovascular Diseases. 2017 Sep 1;26(9):1916–22.
16. Busch K, Chandra R, Buckenham T, Kiat H. Detection of Anomalous Cervical Internal Carotid Artery Branches by Colour Duplex Ultrasound. European Journal of Vascular and Endovascular Surgery. 2017 Jun 1;53(6):776–82.
17. Santos AM, Dos Santos RM, Castro PM, Azevedo E, Sousa L, Tavares JM. A novel automatic algorithm for the segmentation of the lumen of the carotid artery in ultrasound B-mode images. Expert Systems with Applications. 2013 Nov 15;40(16):6570–9.